Investigation of adsorption and mechanism of the cationic methylene blue by the polymeric *Rubia tinctorum* seeds from environment wastewater: kinetic equilibrium and thermodynamic studies

Zineb Wardighi[a], Jaouad Bensalah[a],*, Abdelkader Zarrouk[b], El Housseine Rifi[a], Ahmed Lebkiri[a]

[a]*Laboratory of Advanced Materials and Process Engineering (LAMPE), Department of Chemistry, Faculty of Science, University Ibn Tofail, B.P. 133, 14000, Kenitra, Morocco, emails: Jaouad.bensalah@uit.ac.ma (J. Bensalah) ORCHID: 0000-0001-5758-3559, zineb.wardighi@gmail.com (Z. Wardighi) ORCHID: 0000-0002-4429-1511, elhosseinr@yahoo.fr (E.H. Rifi) ORCHID: 0000-0002-6436-4554, lebkiriahm@yahoo.fr (A. Lebkiri) ORCHID: 0000-0003-0593-0074*
[b]*Laboratory of Materials, Nanotechnology and Environment, Faculty of Sciences, Mohammed V University in Rabat, Av. Ibn Battouta, P.O. Box: 1014 Agdal-Rabat, Morocco, email: azarrouk@gmail.com (A. Zarrouk) ORCHID: 0000-0002-5495-2125*

ABSTRACT

This study focuses on the removal of methylene blue (MB), an organic dye, through adsorption on the *Rubia tinctorum* seeds (RTS) which are considered a new economical and efficient adsorbent for the removal of MB. This efficiency is proven by the microscopic analyses performed using Fourier-transform infrared spectroscopy, X-ray diffraction and scanning electron microscopy/energy-dispersive X-ray spectroscopy analysis techniques. These were performed before and after dye fixation and showed that the prepared surface of the RTS is made up of layers and pores, which could increase the total surface area and provide better fixation for the MB adsorbing cationic dye. To investigate the variation of the adsorption capacity, various parameters were tested such as the mass of the biosorbent, temperature, concentration, pH. The main parameters for maximum adsorption of MB were 40 min contact time and pH 5.00 and a percentage removal of 89.14% was obtained. Under optimal conditions, the monolayer adsorption capacity reached 188.68 mg/g. In addition, modeling studies showed that the adsorption process was best described by the pseudo-second-order kinetic model and the isotherm of Langmuir. Finally, the thermodynamic study revealed the endothermic mode of the MB removal process by RTS.

Keywords: Adsorption; Methylene blue (MB) dye; *Rubia tinctorum*; Kinetics; Thermodynamics; Isotherm

1. Introduction

In recent years, industry has produced various types of toxic contaminants such as dyes, pesticides and heavy metals [1]. These pollutants, discharged into nature, are not only unpleasant for the environment but also affect biological cycles [2]. They can represent a real danger to humans because of their instability and low biodegradability [3]. Dyes are one of the most critical, highly harmful and toxic contaminants produced by industries such as textiles, food, paper, printing, rubber, etc. [4–7]. Among all, the textile industry is one of the biggest consumers of water in the world in addition to using large amounts of various dyes. The annual consumption of all dyes amounts to more than 10.000 tons entering the environment through water [6,8]. These dyes are classified into three groups: anionic, non-ionic and cationic [4].

* Corresponding author.

Methylene blue is one of the most widely used dyes for staining various substrates. It is a basic cationic organic dye, used as a model for the adsorption of organic dyes in aqueous solutions [5]. In the field of wastewater treatment, researchers have made several efforts to develop appropriate methods to control pollution problems using cost-effective wastewater treatment techniques [6]. There are several approaches to removing dyes and other contaminants from wastewater, including sorption, membrane, photocatalytic process, electrochemical and chemical oxidation.

Among them, adsorption has many advantages, such as high performance, low cost, no sludge production, flexibility and ease of implementation. Various adsorbents can be used to eliminate pollutants, including agricultural waste, industrial and municipal waste, activated carbon, hydroxyapatite, clay and water, or natural polymers (chitin, chitosan, alginate, etc.). The use of adsorbents based on natural polymers for the elimination of various contaminants has recently received a great deal of attention [7].

Rubia tinctorum (RTS) is the bioadsorbent used in this work for the removal of methylene blue dye [8]. It has been cultivated for nearly 3.000 y for the dyeing properties of its rhizomes and other properties such as corrosion inhibition and heavy metal adsorption. Following the characterization [9], RTS contains a number of compounds that have been characterized from the roots of *Rubia tinctorum* seeds, in particular *tinctorum* (the source of the commercial color of madder) in addition to alizarin, ruberythric acid, purpurin, lucidin, rubiadin, mollugin, 1-hydroxy-2-methylanthraquinone, the glucosides and/or riversides of these compounds.

The objective of this research is to elaborate on the role of plant-based bioadsorbents for methylene blue (MB) dye removal via the most efficient adsorption method with a critical comparison of the different bioadsorbents through their isothermal, kinetic and thermodynamic studies. The efficient regeneration and removal of other dyes as well as MB has made bioadsorbents a very cost-effective choice for wastewater treatment. These natural adsorbents are extensively modified to increase their surface binding capacity and allow a large number of dye adsorption regeneration cycles.

The novelty of this work consists in using and studying *Rubia tinctorum* seeds in crude form (RTS) as a potential biosorbent for the elimination of methylene blue (MB) as a cationic dye in aqueous solution. The removal capacity was studied as a function of various parameters, namely particle size, adsorbent mass, pH, contact time, initial MB concentration and temperature, respectively. Kinetic and isothermal adsorption models were developed to describe the adsorption mechanism between the biosorbent and the methylene blue cationic dye.

2. Procedure

2.1. Preparation of the adsorbent

The *Rubia tinctorum* seeds studied were collected in the city of Marrakech, Morocco. The preparation of the studied material is made by several steps that are washing with distilled water to remove all impurities, dehydration at a temperature equal to 50°C for 24 h, grinding with an electric grinder and then they were submitted to a sifter with the aim of obtaining the same particle size [10]. The particle size must be less than 250 μm. The particles making up the *Rubia tinctorum* grain powder used in this study were mechanically isolated using a sieve with a mesh size of 250 μm or less (model and manufacturer Fritsch GmbH BRD Industries, Idar-Oberstein). The 250 μm diameter was chosen to favor contact between the support and the dye, because the finer the biosorbent particles, the easier contact with the dye and the higher the adsorption yield. A powder is obtained and washed with distilled water and repeatedly filtered to produce a fine, neat powder [11].

2.2. Preparation of the aqueous solution

The stock solution was prepared by dissolving methylene blue powder (1 g/L) (purchased from Sigma-Aldrich). This solution will be used to prepare other different aqueous solutions containing methylene blue (MB), taking into account their solubility. The concentration of 1 g/L is that of the stock solution of the dye, prepared from its powder. These extraction experiments were carried out using the batch method, with the dose of *Rubia tinctorum* seeds being added to 100 mL of aqueous solution with a known concentration of MB, in several 200 mL conical flasks. Other solutions of HCl and NaOH 10^{-1} mol/L were used to adjust their pH in aqueous solutions [12].

The chemical characteristics and structure of methylene blue are shown in Table 1.

2.3. Chemical assessment of adsorbent material
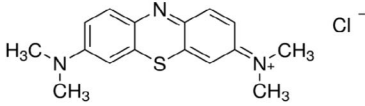
2.3.1. Moisture content

The determination of the percentage of moisture is done by comparing the weight of adsorbent pre m_1 (1 g) and post m_2 (0.88 g) dried in the oven for 48 h at 110°C. The following relationship can be utilized to calculate this factor:

$$H\left(\%\right) = \frac{m_1 - m_2}{m_1} = 12\% \tag{1}$$

2.3.2. Swelling

The phenomenon of swelling of *Rubia tinctorum* seeds can block the use of the material during the conduct of column tests, and it can lead to the clogging of microporous

Table 1
Structure and chemical properties of methylene blue

Properties	Methylene blue
Structure	
Molar mass (g/mol)	319.85
Chemical formula	$C_{16}H_{18}ClN_3S$

filters used for filtration [13]. The swelling percentage can be calculated using the following formula:

$$Q(\%) = \frac{m_2 - m_1}{m_1} \qquad (2)$$

2.3.3. Fourier-transform infrared spectroscopy

The various samples of *Rubia tinctorum* seeds were analyzed by infrared (IRTF), using the spectrometer called (The PerkinElmer Spectrum version 10.03.07), equipped with ALPHA platinum from ATR d a simple reflection and the ATR diamond module. The samples were analyzed without prior preparation [14].

2.3.4. X-ray diffraction

Cellulose is linear and forms intra and intermolecular hydrogen bonds arranged in a regular and ordered system with crystal-like properties. Cellulose is formed of individual fibrillary units consisting of long periods of crystallites interrupted by completely disordered areas, referred to as amorphous [15].

2.3.5. Scanning electron microscopy

The scanning electron microscope allows to obtain images of the surfaces of practically all solid materials, at scales ranging from that of a magnifying glass (x10) to that of transmission electron microscope (x500,000 or more). These images strike first by the very telling rendering of the relief and the great depth of field. The analysis of the surface of the supports studied was carried out using a scanning electron microscope of the VEGA3 TESCAN type [16].

3. Adsorption experiments

MB adsorption was achieved by using the intermission method, the mass of RTS was put in 100 mL of MB solution with predetermined initial concentration, into 200 mL tubes. These bottles were stirred for an optimal time duration, for the purpose of the experiment. The adsorption tests continued at ambient temperature (25°C) [17]. After adsorption testing, the results of the examples were centrifuged at centrifugal laboratory (Hettich Zentifugen, EBA 200) using a spin rate of 5.000 ppm (mg/L) during 5 min for extracting the material of the adsorbent from the solution contains the dye of the cationic MB, and was valued with a spectrophotometer UV-Visible (Selecta P, model-UV-2005) at 664.5 nm.

3.1. Data evaluation

The adsorption of the dye MB by the *Rubia tinctorum* seeds was determined by measuring the efficiency of removal and the adsorbent quantity, respectively shown in Eqs. (3) and (4), with the help of the experimental results [18].

$$R = \frac{C_0 - C_e}{C_0} \times 100 \qquad (3)$$

$$Q_e = \frac{C_0 - C_e}{m} \times V \qquad (4)$$

where C_0: the initial concentration of MB in the solution (mg/L); C_e: the equilibrium concentration of MB in the solution (mg/L); V: the volume of the aqueous solution (L); m: the mass of coriander seeds (g).

4. Results and discussion

4.1. Characterization of the adsorbent

4.1.1. Determination of pH zero charge

The pH_{ZPC} was defined from (Fig. 1) and is equal to value 4.65. The pH_{ZPC} of the bioadsorbent indicates that below this pH, the surface charge of the RTS bioadsorbent is positive and above it, the surface charge is negative. It is not reasonable to adsorb the cationic MB dye in a cationic environment, but if the pH_{ZPC} value is exceeded, better adsorption is obtained. In a strongly acidic environment, well below pH_{ZPC}, the oxygenated sites on the surface of the *Rubia tinctorum* seeds bioadsorbent are hydrogenated and carry a positive charge. In a weakly acidic environment, the hydrogenated sites of the *Rubia tinctorum* seeds bioadsorbent dissociate and neutral sites are formed. At pH_{ZPC}, the surface of the *Rubia tinctorum* seeds (RTS) bioadsorbent is neutral. In a basic environment, at pH ≥ pH_{ZPC}, the hydroxylated functions on the surface of the bioadsorbent dissociate and negatively charged sites appear. The surface of the bioadsorbent thus becomes negative [19,20].

4.1.2. Fourier transform infrared analysis

The attachment of dyes to an adsorbent surface requires the presence of functional groups such as carboxyl, amino, hydroxyl, and other functional groups. To determine the nature of interactions between RTS-MB and different functional groups parties involved in this interaction. The two Fourier-transform infrared (FTIR) spectra are shown in
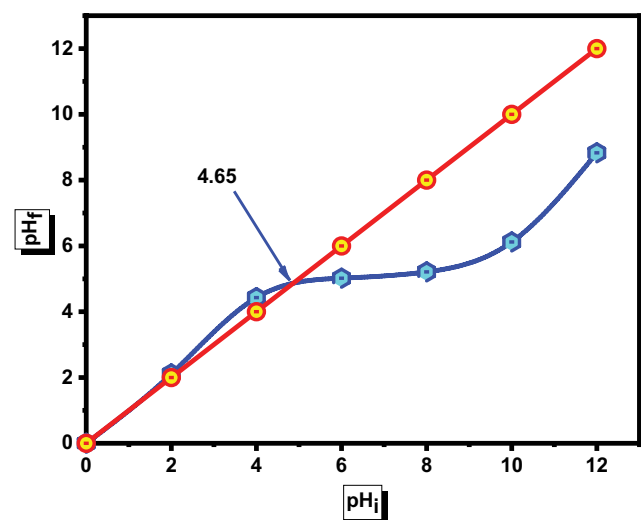

Fig. 1. pH_{PZC} corresponding to the *Rubia tinctorum* seeds.

Fig. 2. The exploited results have already been published in a previous work [21] on the *Rubia tinctorum* seeds brut.

The infrared FTIR spectra obtained from *Rubia tinctorum* seeds (RTS) both before and after the methylene blue adsorption process are illustrated in Fig. 2. Characteristic vibration bands have been attributed to various chemical positions according to data. The spectrum FTIR of data of our support *Rubia tinctorum* seeds, both before and after the additions were nearly identical in format, however, the RTS-MB had a higher degree of intensity [20]. All of the FTIR spectrum showed a large band at 3,340 cm^{-1} that indicates the stretching of OH bonds from aromatic structures with phenolic aliphatic compounds. There is a significant increase in the intensity of the spectra due to the phenomenon of adsorption which leads to asymmetric elongations on the surface of our adsorbent The range around 2,980 cm^{-1} represents the C–H bond asymmetric extension in cellulose. Regarding the group in 2,850 cm^{-1}, it represents a vibration of a symmetrical elongation for the lignin C–H methoxy bonds [21].

However, this peak at 1,733 cm^{-1} indicates the presence of a valence vibration (C=O) due to the carboxylic acid and esters in the hemicelluloses. Moreover, the peak at 1,592 cm^{-1} reflects the C=C shift of the lignin aromatic cycles. Bands at 1,373 cm^{-1}, the value of 1,206 cm^{-1} was due to the vibration ν of (C–O) it is the methoxy radicals of the lignin, the linkage that is created by adsorption phenomenon to cellulose (C–O–C). A peak at 1,013 cm^{-1} represents a vibration of C–O and C–O–C valence bonds in cellulose [22].

4.1.3. Analysis by scanning electron microscopy and energy-dispersive X-ray spectroscopy

Analysis of the surface was carried out with a scanning electron microscopy (SEM) model VEGA3 TESCAN. The micrograph of SEM was obtained from *Rubia tinctorum* seeds before and after the MB removal experiment shown in Fig. 3. In summary, before the adsorption process, the
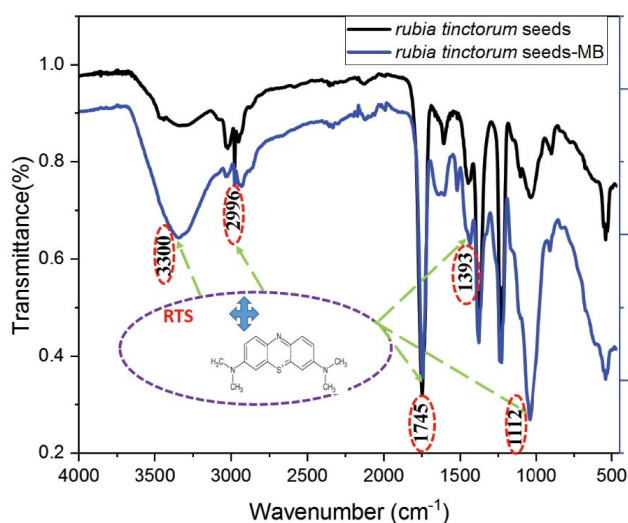

Fig. 2. Fourier-transform infrared spectra of the *Rubia tinctorum* seeds before and after methylene blue polymeric adsorption.

RTS showed a rough surface with several cavities (Fig. 3a) but after adsorption, these cavities were occupied by the studied dye MB (Fig. 3b) [23].

The SEM and energy-dispersive X-ray spectroscopy of the *Rubia tinctorum* seeds both before and after the attachment of the dye can be seen in Fig. 3a and b, accordingly. We can conclude from this fact that the prepared *Rubia tinctorum* seeds surface is made up of coats and pores, which might raise the whole area and provide a better fixation for the cationic adsorbent MB dye. The coats and the pores may be viewed in Fig. 3a which is provided for actively adsorbing the pollutants, whereas Fig. 3b shows the crystals of methylene blue on these pores [24].

4.1.4. X-ray diffraction

The X-ray diffraction (XRD) pattern of *Rubia tinctorum* seeds was shown in Fig. 4. The results obtained show the dominance of the amorphous form, which makes the adsorption possible [25].

The various XRD diagrams of *Rubia tinctorum* seed bark raw materials and sample are given in Fig. 4. On the basis of the published literature, it is apparent that the specimen possesses an amorphous nature; the shape of a natural cellulose is shown as a double peak in Fig. 4; lingo-cellulosic products with a marked dominance of amorphous forms can be described as having no peaks along the spectrum [26].

4.2. Kinetic study

4.2.1. Effect of contact time

To evaluate the effect of contact time on the adsorption of MB by *Rubia tinctorum* seeds, the adsorption experiment was carried out in a solution of MB at room temperature (25°C), solution pH of 5, initial concentration of MB of 10 ppm, and an optimum adsorbent mass of 0.1 g. The experimental results are shown in Fig. 5.

The experiments results showed that the adsorption efficiencies of the dye MB studied on *Rubia tinctorum* seeds increased with increasing contact time. Our biosorbent has achieved the highest rate of the adsorption 89.14% after 40 min. During the initial adsorption phase, there was an increase in the adsorption efficiency due to the presence of many free adsorption sites in *Rubia tinctorum* seeds surface. The pH results obtained from the solution after the extraction tests show that the aqueous environment became less acidic over the course of the extraction operation, resulting in the absorption of H$^+$ ions. From these results, it can be concluded that ions compete with each other and the structure of the dye studied MB to bind to the adsorbent surface [27].

4.2.2. Effect of the adsorbent mass

A study of the effect of mass of the adsorbent on MB adsorption has been conducted by using different amounts of *Rubia tinctorum* seeds and by keeping the other parameters of the experiment constant. The results obtained are shown in Fig. 6. Such results showed that the adsorption efficiency increases with the increase of the adsorbent mass. This increase in *Rubia tinctorum* seeds mass from 0.04 to 1.0 g
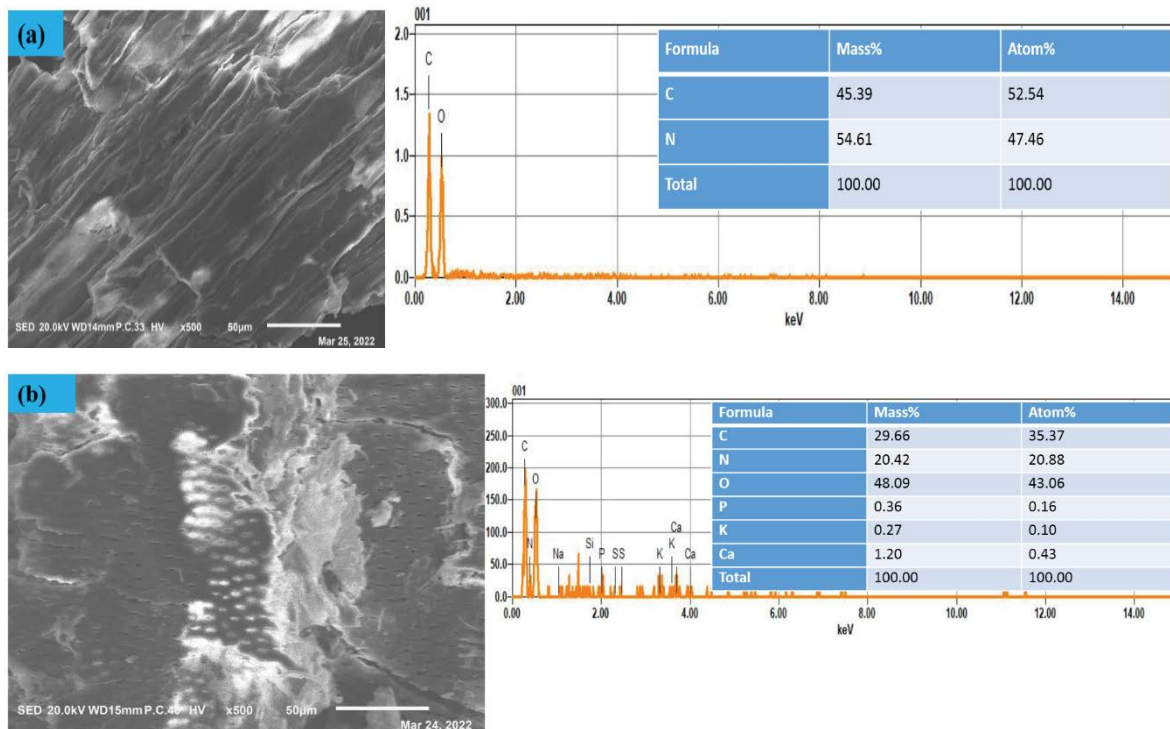
Fig. 3. Micrographs of the scanning electron microscopy/energy-dispersive X-ray spectroscopy of *Rubia tinctorum* seeds both before (a) and after the cationic MB dye adsorption (b).
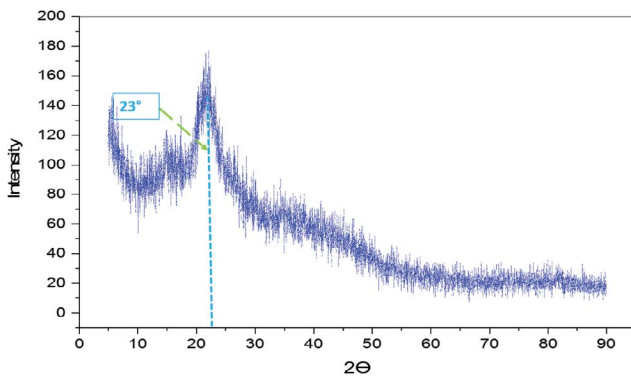

Fig. 4. X-ray spectrum of the *Rubia tinctorum* seeds.

Fig. 5. Impact of time on the concentration of MB dye and the pH of the solution [MB] = 10 mg/L; m = 0.1 g; V = 100 mL; pH_i = 5; T = 298 K; t = 3 h.

indicates that there is an improvement in the adsorption efficiency from 67.92% to 98.88% due to the larger surface arrangement. Increasing *Rubia tinctorum* seeds weight by more than 0.4 g did not result in high adsorption efficiency due to adsorption saturation. Subsequently, the optimal adsorbent weight was chosen at 0.1 g for adsorption efficiency reasons [28].

4.2.3. Effect of the solution pH

The pH of the solution is a factor of great importance that influences the structure of adsorbent, adsorbate, and the adsorption process, it also affects the charge of surface, the circulation and shape of MB molecules. The impact of the solution pH on the adsorption of MB using *Rubia*
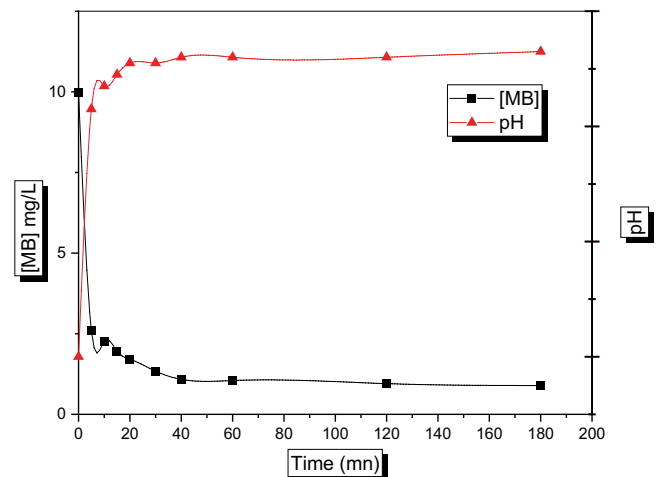
tinctorum seeds was carried out for a pH values between 2 and 12 and the required adjustments were performed using HCl or NaOH (Fig. 7). With a constant dye concentration of 10 ppm, the time of contact was fixed in 2 h with a mass of 0.1 g for *Rubia tinctorum* seeds at ambient temperature 25°C [29]. First change in adsorption yield corresponds to pH values ≤ 5 where a rapid increase in the adsorption rate is noticed. Concerning the pH values between 2 and 6, the adsorption yield continues to increase but with a slower rate, this result probably signifies that the increase
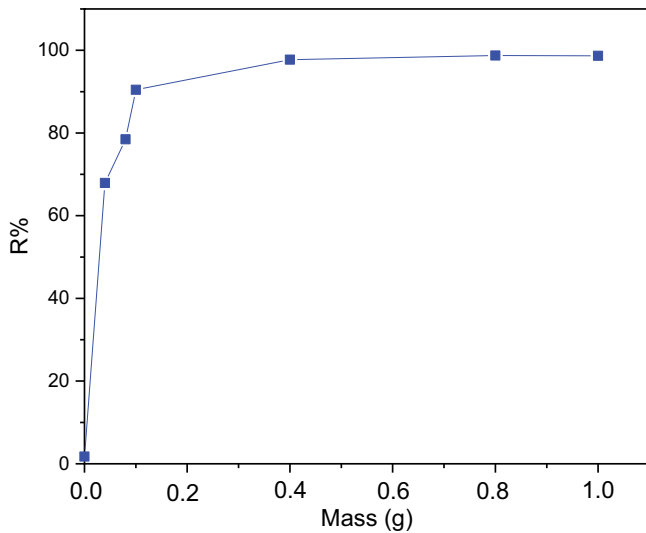
Fig. 6. Impact of the mass of the adsorbent upon the adsorption rate. [MB] = 10 mg/L; V = 100 mL; pH_i = 5; T = 298 K; t = 3 h.

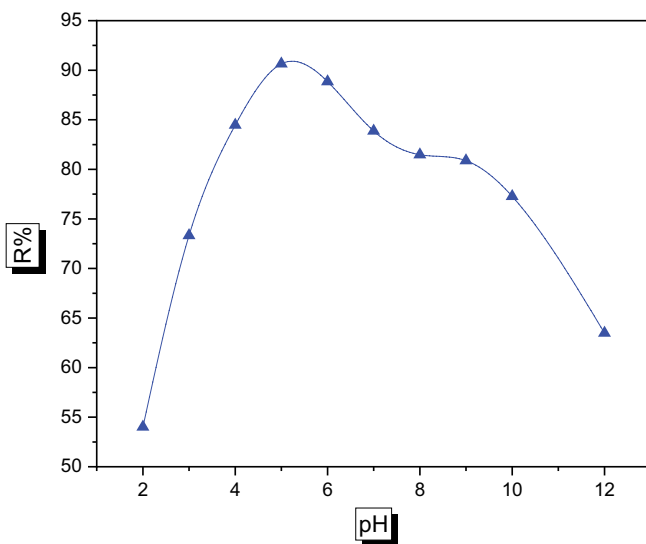Fig. 7. Influence of pH of the adsorbent on the degree of adsorption [MB] = 10 mg/L; V = 100 mL; T = 298 K; m = 0.1 g; t = 3 h.

Fig. 8. Effect of initial [MB] regarding the amount of adsorption. m = 0.1 g; V = 100 mL; pH_i = 5; T = 298 K; t = 3 h.

efficiency up to pH = 5. This explains that the essential mechanism for the adsorption of MB on *Rubia tinctorum* seeds is the electrostatic interaction between them. After the value of 5 the adsorption efficiency decreases until a pH value of 12 which can be explained by the availability of other electrostatic interactions, such as Van Der Waals forces or hydrogen bonds between the dye studied MB and the functional groups of the biosorbent [31].

4.2.4. Effect of the starting concentration of MB dye

In order to determine the influence of the concentration of the cationic adsorbent MB polymeric on the absorption rate, an experiment is made at different concentrations between 10 and 200 mg/L. It was found that adsorption rate for the MB dye by *Rubia tinctorum* seeds grains showed an increase as the initial MB concentration rises to 124.16 from 9.83 mg/g (Fig. 8). These results are explained by the fact that as the concentration is low, the MB molecules have the opportunity to interact with linking points on the adsorbent surface resulting in improved retention efficiency [32].

4.2.5. Effect of temperature

The temperature effect on the amount of adsorption of the MB on the *Rubia tinctorum* seeds has been studied, applying different types of temperatures from 25°C to 65°C. According to Fig. 9, the MB removal efficiency achieved by *Rubia tinctorum* seeds decreases from 90.46% to 78.83%, the temperature varies between 25°C and 65°C, respectively.

These results show that the dye adsorption phenomenon is probably an exothermic one which can be explained by the reason why the temperature increase cannot be promoted through an accumulation of MB on the surface of the solid material [33].

4.2.6. Stirring effect

Stirring speed is a critical factor in adsorption processes. It is involved in the distribution of the adsorbate

of the number of ionized acid functions and subsequently the repulsions of electrostatic nature between the charged sites become significant and also the macromolecular chains become more flexible. Concerning the values higher than 6 we notice a progressive decrease of the adsorption rate, this can be due to the use of NaOH to increase the pH values, the added Na$^+$ cations can play a screen effect between the charged sites. These cations can insert themselves between the macromolecules and decrease the electrostatic repulsions, thus there is compensation between the effect of the increase of the pH value by supporting the ionization of the acid functions and the screen effect induced by NaOH [30].

Separation rates increase as the pH of the initial solution increases from 2 to 5 where RTS is positively charged. Increasing pH is associated with higher MB removal
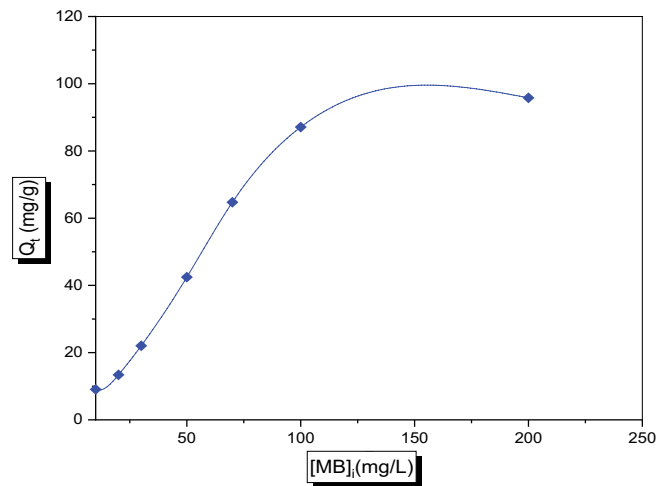
in the adsorption medium and in the determination of the maximum amount adsorbed (Fig. 10). In order to determine the effect of agitation on the adsorption rate, we vary the agitation speed from 100 to 700 (mg/L).

According to the results obtained (Fig. 10), we notice that the adsorption efficiency of the MB dye in the aqueous medium decreases with the increase of the agitation speed. This decrease is probably due to coagulation and also flocculation because of the high speed [34].

4.2.7. Desorption study

The desorption experiment is performed by treating the MB dye-loaded adsorbent samples using 25 mL solutions for 0.1 M NaCl, HCl, NaOH with shaking for 30 min. Every single sample was recovered every minute. The equilibrium MB desorption yield after filtration has been calculated and shown in (Fig. 11) for every agent [35].

The figure shows the most efficient means of desorption of MB from RTS is hydrochloric acid HCl (87.13%) and the least efficient is sodium hydroxide NaOH (23.05%). This result may be interpreted as the RTS-MB responded to the solution of HCl with liberating MB and fixation of protons on RTS surface, while the base of NaOH blocked the desorption of MB by the RTS-MB.

5. Adsorption kinetics

We have applied the pseudo-first-order and second-order to study the experimental results of MB adsorption on *Rubia tinctorum* seeds.

5.1. Pseudo-first-order

The results of the laboratory experiments were interpreted by the pseudo-first-order linear forms of models present [Eq. (5)] [36].

$$\log\left(Q_e - Q_t\right) = \ln\left(Q_e\right) - \frac{K_1}{2.303}t \qquad (5)$$

where Q_e: adsorption quantity at equilibrium (mg/g); Q_t: adsorption quantity of *Rubia tinctorum* seeds at time t (mg/g); K_1: speed constant (min^{-1}).

The model of pseudo-second-order for MB adsorption on the RTS is illustrated in Fig. 12.

5.2. Pseudo-second-order

The kinetic model of pseudo-second-order translates to a linear form as follows [Eq. (6)] [37]:

$$\frac{t}{Q_t} = \frac{t}{Q_e} + \frac{1}{\left(K_2 \cdot Q_e\right)^2} \qquad (6)$$

where Q_e: the amount of MB adsorption at equilibrium (mg/g); Q_t: adsorption quantity of *Rubia tinctorum* seeds at time t (mg/g); K_2: rate constant (g/mg·min).

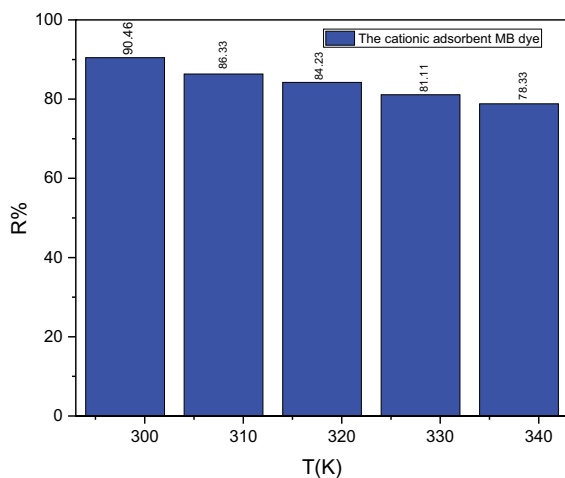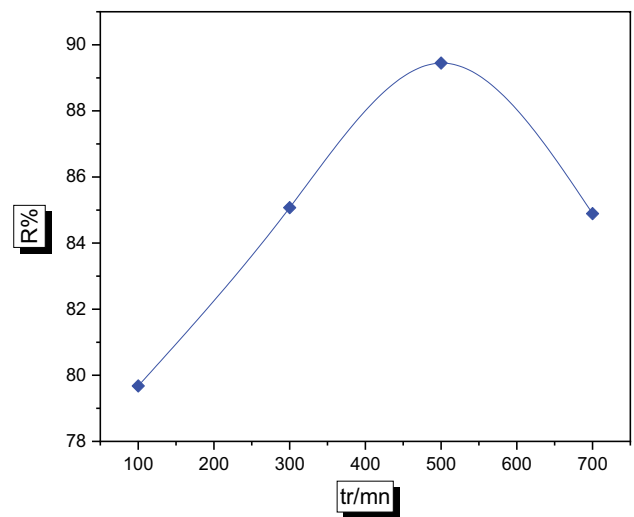Fig. 10. Effect of agitation on the cationic adsorbent MB dye adsorption by *Rubia tinctorum* seeds.

Fig. 9. Impact of temperature on MB dye adsorption by *Rubia tinctorum* seeds. [MB] = 10 mg/L; V = 100 mL; m = 0.1 g; t = 3 h; pH$_i$ = 5.
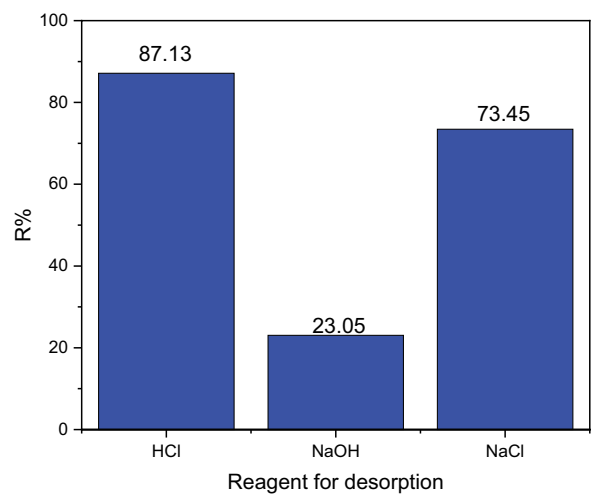

Fig. 11. MB dye desorption from RTS with various desorption agents.

The curve corresponding to the model of pseudo-second-order is in Fig. 13.

From Table 2 we can observe that the coefficient of association R^2 for the second-order kinetic design was unity. In addition, numbers of adsorption capacity obtained by the mathematical simulation studies were similar to the results of the experimental studies. From this remark, it can be concluded that the adsorption of the cationic MB dye by the *Rubia tinctorum* seeds from an aqueous solution followed the pseudo-second-order model [38].
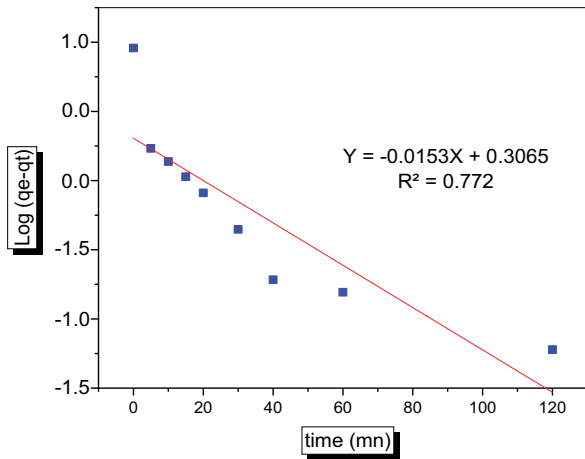

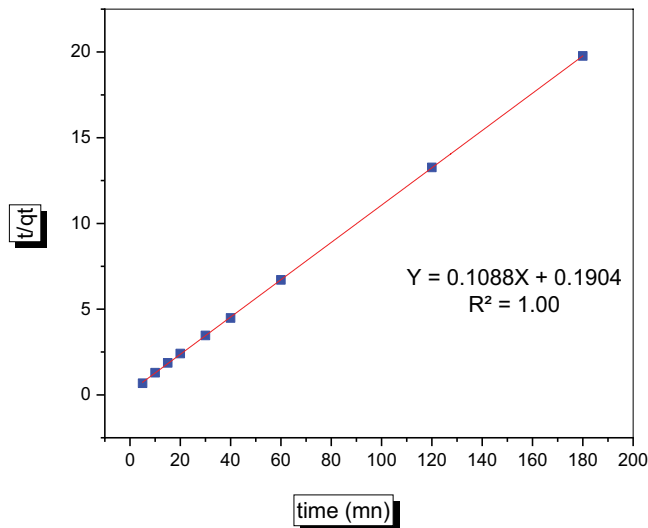Fig. 12. Pseudo-first-order model.

Fig. 13. Pseudo-second-order model.

In conclusion, the adsorption phenomenon is of physical type, with electron exchange between the surface of the adsorbent and the cationic adsorbent MB molecules.

5.3. Elovich model

The Elovich kinetic chemisorption equation Eq. (7) has been used to characterize the adsorption rate which diminishes exponentially with the increase of the amount of adsorbate:

$$\frac{dq_t}{q_t} = \alpha e^{(\beta q_t)} \tag{7}$$

where α (mg/g·min) is the initial adsorption rate and β (g/mg) is the desorption constant related to activation energy for chemisorption. In order to facilitate the Elovich equation, Chein and Clayton [43] applied the border conditions (at $t = 0$, $q_t = 0$) and (at $t = t$, $q_t = q_t$), which given in Eq. (8):

$$Q_t = \frac{1}{\beta}\ln(\alpha\beta) + \frac{1}{\beta}\ln(t) \tag{8}$$

This equation was utilized to correlate our experimental data by plotting the $q_t = f(\ln(t))$ curves. The results are shown in Fig. 14. The constants α, β and R^2 are grouped together in Table 3.

The R^2 values are close to unity, $R^2 < 0.90$ of the MB dye, which confirms that the adsorption is physisorption [44]. The initial adsorption rate of the MB dye on the resins is relatively high, it was between 59.42 mg/g·min, while the MB dye desorption constant decreased from 0.68 in to 10 mg/L of MB.

5.4. Intraparticle diffusion model

The intraparticle diffusion model, also known as the Weber and Morris model [40], has been investigated to demonstrate the MB diffusion process that happens during the adsorption phenomenon between MB dye and *Rubia tinctorum* seeds in Fig. 15.

$$q_t = K_i \times t^{1/2} + \chi_i \tag{9}$$

where q_t: the amount of metal adsorbed on the solid phase is expressed in mg/g; K_i: the slope and concentration value of the junction of the graph curves q_t against $t^{0.5}$ were used to calculate the intraparticle diffusion coefficient (mg/g·min$^{0.5}$).

Table 2
Comparison of first and second-order kinetic models for MB adsorption

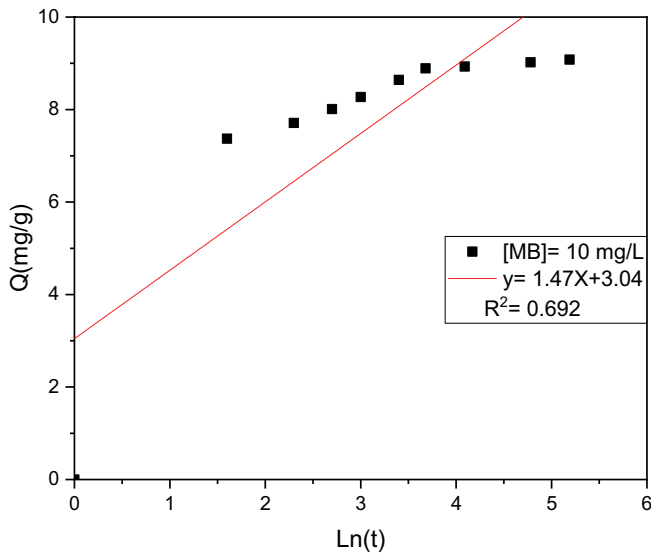| Kinetic model	Parameters			
Pseudo-first-order	Q_{exp} (mg/g)	$Q_{e,cal}$ (mg/g)	K_1 (1/min)	R^2
	9.83	1.35	0.0352	0.7721
Pseudo-second-order	Q_{exp} (mg/g)	$Q_{e,cal}$ (mg/g)	K_2 (1/min)	R^2
	9.83	9.19	0.25	1.00

Fig. 14. Elovich kinetic model for the adsorption of MB dye on *Rubia tinctorum* seeds beads.

Table 3
Kinetic parameters of the Elovich model

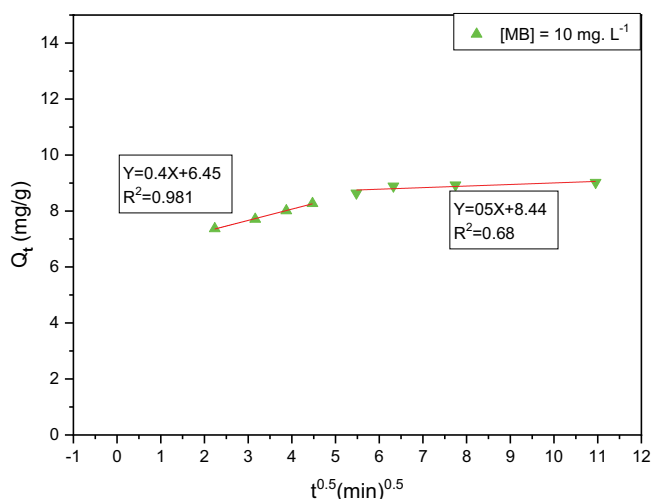| Parameters	[MB]
[MB] mg/L	10
A	59.42
B	0.68
R²	0.692

Fig. 15. Modeling of the kinetics adsorption of MB dye by the model using intraparticle diffusion present.

Table 4 lists the analysis results of adsorption systems cationic MB dye by *Rubia tinctorum* seeds polymeric and the calculated initial factor (R_i). The R_i values are 1 for MB in this table, belonging to zone 0 (no initial adsorption), and are $1 > R_i > 0.9$ for MB, belonging to zone 1 (weakly initial adsorption). The above two zones involve the

Table 4
Parameters study of the intraparticle diffusion

Adsorption of RTS	[MB] (mg/L)	Time (min)	K_i	X_i	R^2
MB	10	<60	0.40	06.45	0.981
		>60	0.05	8.44	0.68

systems using *Rubia tinctorum* seeds as adsorbents in the granular form; the adsorption in these systems is almost the whole process.

The R_i values are $0.9 > R_i > 0.5$ for MB, belonging to zone 2 (intermediately initial adsorption), and are $0.5 > R_i > 0.1$ for MB, belonging to zone 2 (strongly initial adsorption). The group of zones 1 and 2, the main range of adsorption systems. The adsorbents used in zone 1 mainly include powdered *Rubia tinctorum* seeds with a wider pore size distribution. More than half of the adsorption process has an initial behavior. The R_i values are less than 0.1 for the *Rubia tinctorum* seeds where the initial adsorption occupies more than 90% of the adsorption process.

6. Adsorption isotherms

To find out the characteristics of the surface of *Rubia tinctorum* seeds with its adsorption capacity isotherm models were studied [39].

6.1. Langmuir model

The model implies that the adsorption maximum is reached if a satisfied monolayer dye molecules from the solution are installed over the surface of the adsorbent, the adsorption activity of which is constant, and no displacement is made of the absorbed particles in the plane of the surface. We have expressed the linear form by Eq. (10) [40].

$$\frac{C_e}{Q_e} = \frac{1}{K_L Q_m} + \frac{C_e}{Q_m} \tag{10}$$

where C_e: the MB concentration to balance; Q_e: quantity of adsorption (mg/g) to equilibrium; Q_m: the maximal quantity of adsorption (mg/g); K_L: Langmuir constant corresponding to the bound capacity (L/g).

Langmuir isotherm model is illustrated in Fig. 16.

The major characteristic of the model is the constant separation coefficient R_L, which is dimensionless and is calculated by Eq. (11) [41].

$$R_L = \frac{1}{1 + K_L C_{0⊕}} \tag{11}$$

where C_0: the highest concentration of the adsorbate (mg/L); K_L: the Langmuir constant (L/mg).

6.2. Freundlich

The Freundlich equation, which is in linear form and frequently used for adsorption on inhomogeneous surfaces, is shown by Eq. (12) [42]:
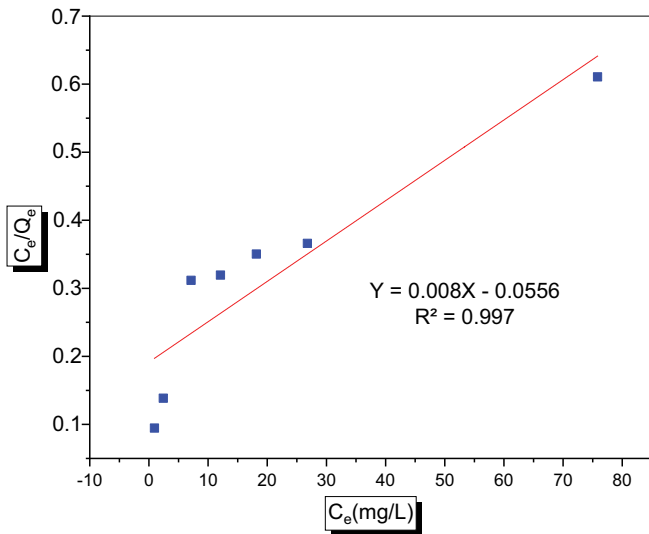
Fig. 16. Isotherm model of Langmuir.

Fig. 17. Freundlich isotherm model.

$$\log(Q_e) = \log(K_F) + \frac{1}{n}\log(C_e) \tag{12}$$

where Q_e: amount of adsorption to balance (mg/g); K_F: Freundlich constant (L/g); C_e: the MB ion concentration value at equilibrium (mg/L).

The size of $1/n$ indicates a favorable adsorption character, $n > 1$ represents a favorable adsorption condition [43].

K_F and n are determined from the Freundlich curve shown in Fig. 17.

The parameters that characterize each isothermal model are presented in Table 3.

6.3. Temkin

The isothermal equation of Temkin supposes that the heat of adsorption of all molecules in the aqueous solution of cationic dye MB diminishes linearly with coverage because of adsorbent–adsorbate interactions, and that adsorption is characterized by an orderly allocation of binding energies, up to a maximum binding energy [30]. The linear form of this isotherm model can be presented using the following equation:

$$q_t = B_1 \ln(K_T) + B_1 \ln(C_e) \tag{13}$$

The concentration of the cationic resin at equilibrium (mg/L), q_e is the capacity of adsorbent adsorbed at equilibrium (mg/g), $RT/\Delta Q = B_1$ whither T is the temperature (K), and R is the typical gas constant (8.314 J/mol·K) and ΔQ is the diversity of the adsorption energy.

A linear plot of Q_e vs. C_e shown in Fig. 18 allows the determination of the parameters. The constant ΔQ is related to the heat of adsorption. The values of A and B_1 are included in Table 5. Therefore, the process of adsorption of MB dye on *Rubia tinctorum* seeds can be summary as physisorption, as presented by the value of (ΔQ) which is more than 40 kJ/mol [31].
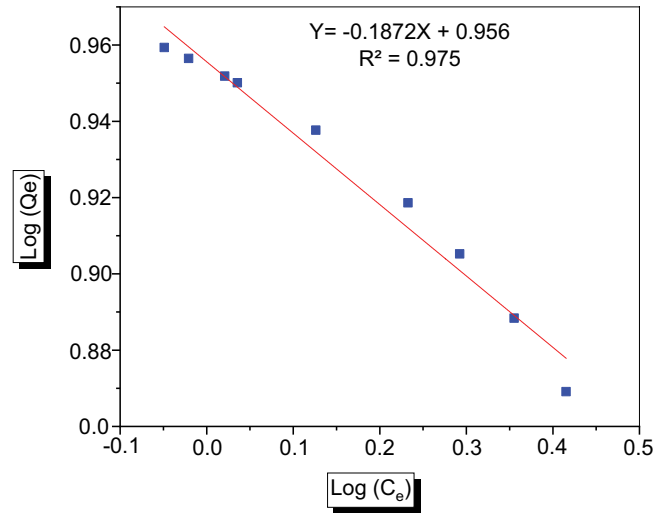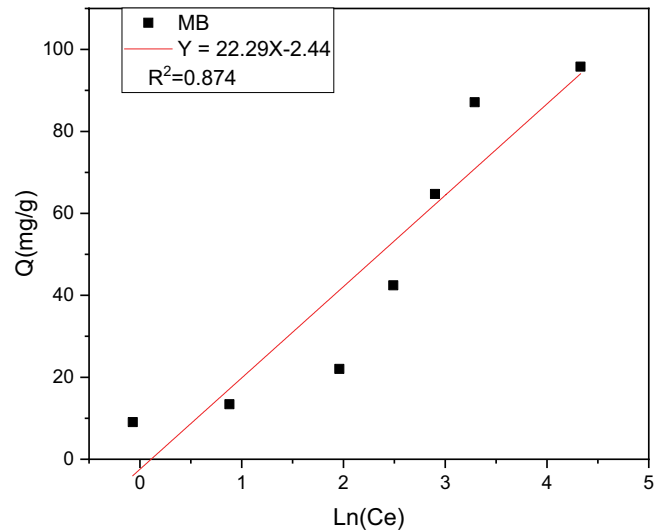

Fig. 18. Temkin of MB adsorption on *Rubia tinctorum* seeds.

Based on the diagram of the individual isotherm (Fig. 17, Table 5), showing both the correlation ($R^2 = 0.997$) values as well as the values of the constants of the individual model, the retention process of the cationic adsorbent MB dye polymeric is evidently shown in the Langmuir model, therefore, based on the Freundlich and Temkin model, the solid adsorbent has a finite capacity of adsorption (q_m), and all its active locations are equal($Q_{m\text{-}exp} = Q_{m\text{-}cal} = 125$ mg/g), meaning it can only complex a single molecule of solute. In addition, there is no interaction among adsorbed molecules [44].

7. Thermodynamic studies

For an adsorption process, it is necessary to make a thermodynamic study in order to give a description of a process. Required variables like free energies ($\Delta G°$), enthalpies ($\Delta H°$) and entropy ($\Delta S°$) may be calculated using balance values, varying with temperature [45].

Table 5
Parameters of adsorption isotherm model

Isothermal models	Parameters	
Langmuir	$Q_{m\text{-cal}}$ (mg/g)	125.00
	$Q_{m\text{-exp}}$ (mg/g)	124.16
	K_L (L/mg)	–0.145
	R_L	–0.035
	R^2	0.997
Freundlich	K_F (mg/g)	2.60
	n	–5.341
	R^2	0.975
Temkin	B_1	22.29
	ΔQ (kJ/mol)	0.111
	K_T	0.89
	R^2	0.874

$\Delta G°$, the change in standard free energy (J) can be calculated as follows [Eq. (14)] [46]:

$$\Delta G° = -RT \ln\left(K_D\right) \tag{14}$$

where R: constant of universal gas (8.314 J/mol·K); T: ambient temperature (298 K); K_D: constant of thermodynamic equilibrium (L/g), which is stated by Eq. (15).

$$K_D = \left(\frac{Q_e}{C_e}\right) \tag{15}$$

where Q_e: quantity of adsorbed MB dye to equilibrium (mg/g); C_e: equilibrium MB concentration in the total system (mg/L).

The rates for $\Delta H°$ and $\Delta S°$ were calculated by curving and intercepting $\ln(K_D)$ vs. $1/T$ (Fig. 19) by Eq. (16) [46]:

$$\ln\left(K_D\right) = -\frac{\Delta H°}{RT} + \frac{\Delta S°}{R} \tag{16}$$

$\Delta G°$, $\Delta H°$ and $\Delta S°$ are associated by Eq. (17):

$$\Delta G° = \Delta H° - T\Delta S° \tag{17}$$

The Van't Hoff diagram representing the MB adsorption process by the *Rubia tinctorum* seeds is given in Fig. 19.

The thermodynamic parameters are mentioned in Table 6. The value of $\Delta H°$ affirms that the process of adsorption is exothermic. Moreover, the values of $\Delta G°$, $\Delta S°$ showed that MB dye retention process by *Rubia tinctorum* seeds means that we have two mechanisms, adsorption and ion transfer [46].

8. Comparative study

Discussion of the performance of different groups of adsorbents that have been used by researchers in recent years to attenuate MB from aqueous solutions is shown in
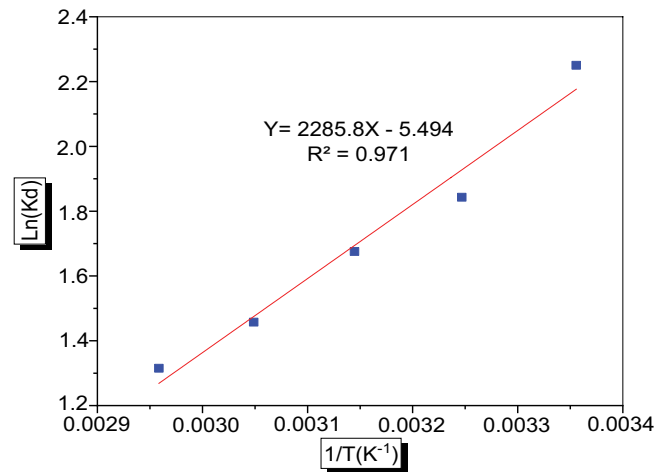

Fig. 19. Van't Hoff curve showing the cationic adsorbent MB dye adsorption by *Rubia tinctorum* seeds.

Table 6
Thermodynamic parameters of the adsorption of MB on RTS

Temperature (K)	K_D (L/g)	$\Delta G°$ (kJ/mol)	$\Delta H°$ (kJ/mol)	$\Delta S°$ (J/mol·K)
298	9.50	–5.59		
308	6.31	–5.14		
318	5.34	–4.69	–19.004	–0.045
328	4.30	–4.24		
338	3.72	–3.79		

Table 7
A previous study of the MB adsorption using various natural adsorbents

Adsorbent	Adsorption capacity (mg/g)	References
Rough reed fibers (R)	21.01	[49]
Coriandrum sativum seeds	107.53	[50]
Carica papaya	32.25	[51]
Rubia tinctorum seeds	124.16	Present work
Treated reed fibers (RS)	54.73	[52]

Table 7. Many examples of adsorbents are rough reed fibers, *Coriandrum sativum*, *Carica papaya*, *Rubia tinctorum* seeds, treated reed fibers. According to Table 7, the most effective biosorbent for the adsorption of MB dye is *Rubia tinctorum* seeds. This can be explained by the fact that it is perceived as having a high adsorption capacity. These findings encourage to try *Rubia tinctorum* seeds as a low-cost natural carrier to remove the cationic adsorbent MB dye from wastewater. Other groups of adsorbents also used are *Coriandrum sativum* seeds, which can be explained by their growing popularity due to their very small size. This contributes to their high surface area, which invariably increases their adsorption capacity. Reed fibers, treated reed fibers and
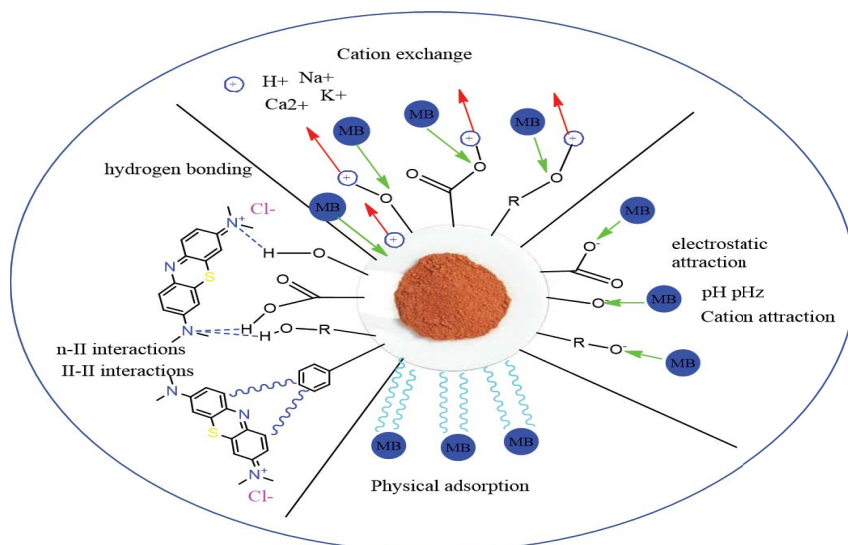
Fig. 20. Mechanisms of ionic and electrostatic interaction.

Carica papaya are another group of adsorbents that have been frequently used for the same purpose of MB dye adsorption in recent years. This may be due to their ability to adsorb water in their interlayer sites and their high surface area, which are the properties of a good adsorbent [48].

9. Other possible mechanisms of biosorption

A presence of –OH groups affects the adsorption mechanism. On the other hand, cationic properties of methylene blue showed that they relocate the load. These groups may be present in either sulphates or in nitrogen. They are of course, most often present on the nitrogen atom. Since the carboxyl radicals are found to adsorb the loaded dye at such pH values > pH_{PZC}, the biosorbent surface has a negative charge due to the COO^- [45].

A presence of –OH functional groups, together with the existence of double free electrons from the nitrogen atoms of the dye, are visible in FTIR analysis (Fig. 20). The sulphuric atoms were found to have similar behavior in Fig. 20. The proposed process consists of electrostatic interaction and creation of hydrogen bonds, donor-acceptor electron exchange interactions, and dispersive π–π interaction [45].

10. Conclusion

The experiments in this study showed that *Rubia tinctorum* seeds were excellent at removing the MB cationic adsorbent dye from synthetic solutions, and with SEM, FTIR analysis, it is shown that RTS is capable of extracting the MB dye from the aqueous phase using adsorption. The equilibrium point was reached as the contact time was 40 min. The various parameters influencing the adsorption process were examined, including adsorbent mass, pH, initial MB concentration and temperature. According to the RSM analysis of experimental factors, tests with 10 mg of adsorbent, 40 min of contact time and an initial dye concentration of 10 mg/L for MB were carried out under ideal conditions to obtain the greatest dye removal.

The maximum adsorption capacity was 124.16 mg/g and the adsorption processes were in good agreement with the pseudo-second-order kinetics and Langmuir isotherm models. The kinetic analyses affirm that the process is consistent with a pseudo-second-order model. The values of $\Delta G°$, $\Delta H°$, and $\Delta S°$ that were submitted by the thermodynamic experiments that the adsorption process on the RTS surface is stable and exothermic. This research has shown that the last-mentioned adsorbent is a low-cost support and can be used to adsorb MB dye present in waste.

Disclosure statement

No potential conflict of interest was reported by the authors.

References

[1] H. Jia, Z. Sun, G. Li, A four-stage constructed wetland system for treating polluted water from an urban river, Ecol. Eng., 71 (2014) 48–55.

[2] M. Lapuerta, R. Ballesteros, F.J. Martos, A method to determine the fractal dimension of diesel soot agglomerates, J. Colloid Interface Sci., 303 (2006) 149–158.

[3] A.M. Ghaedi, M. Ghaedi, A. Vafaei, N. Iravani, M. Keshavarz, M. Rad, I. Tyagi, S. Agarwal, V.K. Gupta, Adsorption of copper(II) using modified activated carbon prepared from pomegranate wood: optimization by bee algorithm and response surface methodology, J. Mol. Liq., 206 (2015) 195–206.

[4] A. Ahmadi, R. Foroutan, H. Esmaeili, S.J. Peighambardoust, S. Hemmati, B. Ramavandi, Montmorillonite clay/starch/ $CoFe_2O_4$ nanocomposite as a superior functional material for uptake of cationic dye molecules from water and wastewater,

Mater. Chem. Phys., 284 (2022) 126088, doi: 10.1016/j. matchemphys.2022.126088.

[5] R. Foroutan, R. Mohammadi, N. Sohrabi, S. Sahebi, S. Farjadfard, Z. Esvandi, B. Ramavandi, Calcined alluvium of agricultural streams as a recyclable and cleaning tool for cationic dye removal from aqueous media, Environ. Technol. Innovation, 17 (2020) 100530, doi: 10.1016/j.eti.2019.100530.

[6] K. Karami, F. Mehvari, V. Ramezanzade, M. Zakariazadeh, M. Kharaziha, A. Ramezanpour, The interaction studies of novel imine ligands and palladium(II) complexes with DNA and BSA for drug delivery application: the anti-cancer activity and molecular docking evaluation, J. Mol. Liq., 362 (2022) 119493, doi: 10.1016/j.molliq.2022.119493.

[7] R. Foroutan, S.J. Peighambardoust, H. Aghdasinia, R. Mohammadi, B. Ramavandi, Modification of bio-hydroxyapatite generated from waste poultry bone with MgO for purifying methyl violet-laden liquids, Environ. Sci. Pollut. Res., 27 (2020) 44218–44229.

[8] M. Noori, M. Tahmasebpoor, R. Foroutan, Enhanced adsorption capacity of low-cost magnetic clinoptilolite powders/beads for the effective removal of methylene blue: adsorption and desorption studies, Mater. Chem. Phys., 278 (2022) 125655, doi: 10.1016/j.matchemphys.2021.125655.

[9] Z. Jin, S. Deng, Y. Wen, Y. Jin, L. Pan, Y. Zhang, T. Black, K.C. Jones, H. Zhang, D. Zhang, Application of *Simplicillium chinense* for Cd and Pb biosorption and enhancing heavy metal phytoremediation of soils, Sci. Total Environ., 697 (2019) 134148, doi: 10.1016/j.scitotenv.2019.134148.

[10] Y. Wang, Y. Xie, Y. Zhang, S. Tang, C. Guo, J. Wu, R. Lau, Anionic and cationic dyes adsorption on porous poly-melamine-formaldehyde polymer, Chem. Eng. Res. Des., 114 (2016) 258–267.

[11] M.A. Maisyarah, L.J. Shiun, A. Fa. Nasir, H. Haslenda, H.W. Shin, Characteristics of cellulose, hemicellulose and lignin of MD2 pineapple biomass, Chem. Eng. Trans., 72 (2019) 79–84.

[12] J. Kurek, P. Kwaśniewska-Sip, K. Myszkowski, T. Pospieszny, W. Pietruś, G. Cofta, P. Barczyński, M. Murias, Alkaloid from *Colchicum* species in complexes with lithium, sodium, potassium and magnesium cations–spectroscopic characterization, semiempirical and theoretical calculation, fungicidal and cytotoxic activity, J. Mol. Struct., 1204 (2020) 127520, doi: 10.1016/j.molstruc.2019.127520.

[13] A. Ronda, M.A. Martín-Lara, M. Calero, G. Blázquez, Analysis of the kinetics of lead biosorption using native and chemically treated olive tree pruning, Ecol. Eng., 58 (2013) 278–285.

[14] J. Bensalah, M. Berradi, A. Habsaoui, O. Dagdag, A. El Amri, O. El Khattabi, A. Lebkiri, E.H. Rifi, Adsorption of the orange methyl dye and lead(II) by the cationic resin Amberlite®IRC-50: kinetic study and modeling of experimental data, J. Chem. Soc. Pak., 43 (2021) 535–545.

[15] J. Bensalah, M. Berradi, A. Habsaoui, M. Allaoui, H. Essebaai, O. El Khattabi, A. Lebkiri, E.H. Rifi, Kinetic and thermodynamic study of the adsorption of cationic dyes by the cationic artificial resin Amberlite®IRC50, Mater. Today Proc., 45 (2021) 7468–7472.

[16] J. Bensalah, A. Habsaoui, B. Abbou, L. Kadiri, I. Lebkiri, A. Lebkiri, E.H. Rifi, Adsorption of the anionic dye methyl orange on used artificial zeolites: kinetic study and modeling of experimental data, Mediterr. J. Chem., 9 (2019) 311–316.

[17] J. Bensalah, A. Habsaoui, O. Dagdag, A. Lebkiri, I. Ismi, E.H. Rifi, I. Warad, A. Zarrouk, Adsorption of a cationic dye (safranin) by artificial cationic resins Amberlite®IRC-50: equilibrium, kinetic and thermodynamic study, Chem. Data Collect., 35 (2021) 100756, doi: 10.1016/j.cdc.2021.100756.

[18] J. Bensalah, A. Habsaoui, A. Lebkiri, O. El Khattabi, E.H. Rifi, Investigation of the cationic resin Amberlite®IRC-50 as a potential adsorbent to remove the anionic dye methyl orange, Desal. Water Treat., 246 (2022) 280–290.

[19] E.M. Cafferty, Relationship between the isoelectric point (pH_{PZC}) and the potential of zero charge (E_{pzc}) for passive metals, Electrochim. Acta, 55 (2010) 1630–1637.

[20] K. Naseem, Z.H. Farooqi, R. Begum, M.Z. Ur Rehman, A. Shahbaz, U. Farooq, M. Ali, H.M.A. Ur Rahman, A. Irfan, A.G. Al-Sehemi, Removal of cadmium(II) from aqueous medium using *Vigna radiata* leave biomass: equilibrium isotherms, kinetics and thermodynamics, Z. Phys. Chem., 235 (2019) 669–690.

[21] Z. Wardighi, A. EL Amri, L. Kadiri, A. Jebli, F.Z. Bouhassane, E.H. Rifi, A. Lebkiri, Ecological study of elimination of the organic pollutant (violet crystal) using natural fibers of *Rubia tinctorum*: optimization of adsorption processes by BBD-RSM modeling and DFT approaches, Inorg. Chem. Commun., 155 (2023) 111014, doi: 10.1016/j.inoche.2023.111014.

[22] N. Fayoud, S.A. Younssi, S. Tahiri, A. Albizane, Kinetic and thermodynamic study of the adsorption of methylene blue on wood ashes, Mor. J. Chem., 6 (2015) 3295–3306.

[23] M.A. Dia, S.M. Lo, M. Pontié, H. Bagan, C.K. Diawara, M. Rumeau, Feasibility study of a new water softening process by ion exchange for domestic use, C.R. Chim., 9 (2006) 1260–1267.

[24] J. Bensalah, A. El Amri, A. Ouass, O. Hammani, L. Kadiri, H. Ouaddari, E.M. Saaoudi, A. Zarrouk, B. Srhir, Investigation of the cationic resin Am®IRC-50 as a potential adsorbent of Co(II): equilibrium isotherms and thermodynamic studies, Chem. Data Collect., 39 (2022) 100879, doi: 10.1016/j.cdc.2022.100879.

[25] A. El Amri, R. Hsisou, A. Jebli, I. Lebkiri, J. Bensalah, F.Z. Bouhassane, L. Alami, A. Lebkiri, A. Zarrouk, E.H. Rifi, A. Lebkiri, Acid activation of natural reed filter biomass (*Typha latifolia*) application to Pb(II) uptake from aqueous solutions: kinetic, thermodynamic equilibrium studies and optimization studies, Chem. Afr., (2023), doi: 10.1007/s42250-023-00733-0.

[26] K. Naseem, Z.H. Farooqi, R. Begum, M.Z. Ur Rehman, M. Ghufran, W. Wu, J. Najeeb, A. Irfan, Synthesis and characterization of poly(N-isopropylmethacrylamide-acrylic acid) smart polymer microgels for adsorptive extraction of copper(II) and cobalt(II) from aqueous medium: kinetic and thermodynamic aspects, Environ. Sci. Pollut. Res., 27 (2020) 28169–28182.

[27] J. Bensalah, F. Benhiba, A. Habsaoui, A. Ouass, A. Zarrouk, A. Lebkiri, O. El Khattabi, E.H. Rifi, The adsorption mechanism of the anionic and cationic dyes of the cationic resin A®IRC-50, kinetic study and theoretical investigation using DFT, J. Indian Chem. Soc., 99 (2022) 100512, doi: 10.1016/j.jics.2022.100512.

[28] Z. El Kerdoudi, J. Bensalah, H. Helli, A. El Mekkaoui, N. EL Mejdoub, Investigation of the cationic dye methylene blue in the treatment of wastewater clay from Sidi-Kacem (Morocco): kinetic and mathematical modelling of experimental data, Mater. Today Proc., 72 (2023) 3550–3555.

[29] J. Henschen, D. Li, M. Ek, Preparation of cellulose nanomaterials via cellulose oxalates, Carbohydr. Polym., 213 (2019) 208–216.

[30] B. Abbou, I. Lebkiri, H. Ouaddari, L. Kadiri, A. Ouass, A. Elamri, J. Bensalah, A. Habsaoui, A. Lebkiri, E.H. Rifi, Study of the adsorption performance of a cationic dye onto a Moroccan clay, J. Chem. Health Risks, 11 (2021), doi: 10.22034/jchr.2021.1922221.1252.

[31] M. Elabboudi, J. Bensalah, A. El Amri, N. EL Azzouzi, B. Srhir, A. lebkiri, A. Zarrouk, E.H. Rifi, Adsorption performance and mechanism of anionic MO dye by the adsorbent polymeric Amberlite®IRA-410 resin from environment wastewater: equilibrium kinetic and thermodynamic studies, J. Mol. Struct., 1277 (2023) 134789, doi: 10.1016/j.molstruc.2022.134789.

[32] M. EL Alouani, S. Alehyen, M. EL Achouri, M. Taibi, Removal of cationic dye – methylene blue - from aqueous solution by adsorption on fly ash-based geopolymer, J. Mater. Environ. Sci., 9 (2018) 32–46.

[33] S. Elbariji, M. Elamine, H. Eljazouli, H. Kabli, A. Lacherai, A. Albourine, Treatment and recovery of wood by-products. Application to the elimination of industrial dyes, C.R. Chim., 9 (2006) 1314–1321.

[34] M. Basu, A.K. Guha, L. Ray, Adsorption behavior of cadmium on husk of lentil, Process Saf. Environ. Prot., 106 (2017) 11–22.

[35] L. Li, L. Fan, M. Sun, H. Qiu, X. Li, H. Duan, C. Luo, Adsorbent for hydroquinone removal based on graphene oxide

functionalized with magnetic cyclodextrin–chitosan, Int. J. Biol. Macromol., 58 (2013) 169–175.

[36] A. Saravanan, P. Senthil Kumar, M. Govarthanan, C.S. George, S. Vaishnavi, B. Moulishwaran, S. Praveen Kumar, S. Jeevanantham, P.R. Yaashikaa, Adsorption characteristics of magnetic nanoparticles coated mixed fungal biomass for toxic Cr(VI) ions in aquatic environment, Chemosphere, 267 (2021) 129226, doi: 10.1016/j.chemosphere.2020.129226.

[37] M. Allaoui, M. Berradi, J. Bensalah, H. Es-Sahbany, O. Dagdag, S. Ibn Ahmed, Study of the adsorption of nickel ions on the seashells of Mehdia: kinetic and thermodynamic study and mathematical modelling of experimental data, Mater. Today Proc., 45 (2021) 7494–7500.

[38] M. Allaoui, M. Berradi, H. Taouil, H. Es-Sahbany, L. Kadiri, A. Ouass, J. Bensalah, S. Ibn Ahmed, Adsorption of heavy metals (nickel) by the shell powder of the coast of Mehdia-Kenitra (Morocco), Anal. Bioanal. Electrochem., 11 (2019) 1547–1558.

[39] Y. Essaadaoui, A. Lebkiri, E. Rifi, L. Kadiri, A. Ouass, Adsorption of lead by modified *Eucalyptus camaldulensis* barks: equilibrium, kinetic and thermodynamic studies, Desal. Water Treat., 111 (2018) 267–277.

[40] S. Agarwal, I. Tyagi, V.K. Gupta, M.H. Dehghani, J. Jaafari, D. Balarak, M. Asif, Rapid removal of noxious nickel(II) using novel γ-alumina nanoparticles and multiwalled carbon nanotubes: kinetic and isotherm studies, J. Eng. Environ. Sci., 32 (2008) 303–312.

[41] A. Sadeghizadeh, F. Ebrahimi, M. Heydari, M. Tahmasebi-kohyani, F. Ebrahimi, A. Sadeghizadeh, Adsorptive removal of Pb(II) by means of hydroxyapatite/chitosan nanocomposite hybrid nanoadsorbent: ANFIS modeling and experimental study, J. Environ. Manage., 232 (2019) 342–353.

[42] S. Şimşek, Adsorption properties of lignin containing bentonite–polyacrylamide composite for ions, Desal. Water Treat., 57 (2016) 23790–23799.

[43] S. Klas, D.W. Kirk, Advantages of low pH and limited oxygenation in arsenite removal from water by zero-valent iron, J. Hazard. Mater., 252–253 (2013) 77–82.

[44] K. Azoulay, I. Bencheikh, A. Moufti, A. Dahchour, J. Mabrouki, S. El Hajjaji, Comparative study between static and dynamic adsorption efficiency of dyes by the mixture of palm waste using the central composite design, Chem. Data Collect., 27 (2020) 100385, doi: 10.1016/j.cdc.2020.100385.

[45] N. Balkıs, Y. Aktan, N. Balkıs, Toxic metal (Pb, Cd and Hg) levels in the nearshore surface sediments from the European and Anatolian Shores of Bosphorus, Turkey, Mar. Pollut. Bull., 64 (2012) 1938–1939.

[46] J. Bensalah, M. Galai, M. Ouakki, A. El Amri, B. Hanane, A. Habsaoui, O. EL Khattabi, A. Lebkiri, A. Zarrouk, E.H. Rifi, A combined experimental and thermodynamics study of mild steel corrosion inhibition in 1.0 M hydrochloric solution by the cationic polymer Amberlite®IRC-50 resin extract, Chem. Data Collect., 43 (2023) 100976, doi: 10.1016/j.cdc.2022.100976.

[47] A. Sihem, M.B. Lehocine, H.A. Miniai, Preparation and characterisation of an natural adsorbent used for elimination of pollutants in wastewater, Energy Procedia, 18 (2012) 1145–1151.

[48] L. Kadiri, A. Ouass, Y. Essaadaoui, E.H. Rifi, A. Lebkiri, *Coriandrum sativum* seeds as a green low-cost biosorbent for methylene blue dye removal from aqueous solution: spectroscopic, kinetic and thermodynamic studies, Mediterr. J. Chem., 7 (2018) 204–216.

[49] A. El Amri, J. Bensalah, A. Idrissi, L. Kadiri, A. Ouass, S. Bouzakraoui, A. Zarrouk, E.H. Rifi, A. Lebkiri, Adsorption of a cationic dye (methylene bleu) by *Typha latifolia*: equilibrium, kinetic and DFT calculations, Chem. Data Collect., 38 (2022) 100834, doi: 10.1016/j.cdc.2022.100834.

[50] A. EL Amri, J. Bensalah, Y. Essaadaoui, I. Lebkiri, B. Abbou, A. Zarrouk, E.H. Rifi, A. Lebkiri, Elaboration, characterization and performance evaluation of a new environmentally friendly adsorbent material based on the reed filter (*Typha latifolia*): kinetic and thermodynamic studies and application in the adsorption of Cd(II) ion, Chem. Data Collect., 39 (2022) 100849, doi: 10.1016/j.cdc.2022.100849.

[51] J. Li, Z. Wang, J. Wang, J. Gao, M. Zou, Y. Li, B. Wang, L. Xia, Spectroscopic investigation on the sonodynamic activity of Safranine T to bovine serum albumin damage, J. Lumin., 132 (2012) 282–288.

[52] J. Jaafari, K. Yaghmaeian, Response surface methodological approach for optimizing heavy metal biosorption by the blue-green alga *Chroococcus disperses*, Desal. Water Treat., 142 (2019) 225–234.